# Theoretical study on the effect of an O vacancy on the hydrogen storage properties of the LaFeO₃ (010) surface

*Yuhong Chen* (陈玉红)[a,b,*], *Jiajia Fan* (范嘉佳)[a,b], *Tingting Liu* (刘婷婷)[a,b], *Jing Wang* (王敬)[a,b], *Meiling Zhang* (张梅玲)[b,c], *Cairong Zhang* (张材荣)[a,b]

[a] *State Key Laboratory of Advanced Processing and Recycling of No-ferrous Metals, LanZhou University of Technology, Lanzhou 730050, China*
[b] *School of Science, Lanzhou University of Technology, Lanzhou 730050, China*
[c] *The School of Nuclear Science and Technology, Lanzhou University, Lanzhou 730000, China*

## ARTICLE INFO

## ABSTRACT

Based on first-principles calculations, we investigated the hydrogen adsorption dissociation on the LaFeO₃ (010) surface with an O vacancy. It was confirmed that $H_2$ molecules have four kinds of adsorption modes on LaFeO₃ (010) surfaces with an O vacancy. First, H atoms are adsorbed on O atoms to form an —OH group. Second, H atoms are adsorbed on Fe atoms to form Fe—H bonds. Third, two H atoms are adsorbed on the same O atom to form $H_2O$. Fourth, two H atoms are adsorbed on the same Fe atom and it is a new type of adsorption, which does not exist in the ideal surface. The main channel of dissociative adsorption is the fourth adsorption mode of —OH and Fe—H, where the H atoms adsorbed on the surface of Fe can be easily diffused into O atoms. Charge population analysis showed that increasing the O vacancy enhanced the interaction between Fe—H. In the system containing O vacancies adsorbed H atoms in the top of Fe to diffuse to the top of O need to overcome the energy barrier decreased from 0.968 eV to 0.794 eV. So the existence of an O vacancy enhances the hydrogen absorption properties of Fe atoms in LaFeO₃.

## Introduction

With the rapid development of portable electronic products, communication equipment, hybrid cars, and other high-tech products, the electrochemical performance of NiMH batteries requires higher capacity and lower cost, and therefore, studies that explore and investigate new anode materials having a high specific energy are one of the keys to achieve a high-energy nickel hydrogen battery [1]. The traditional cathode materials for Ni/MH batteries are hydrogen storage alloys, which have presented some problems in electrode capacity, activation properties, kinetic properties, cycle life, and material cost. Therefore, research on new anode materials has remained ongoing. ABO₃ perovskite oxide can be used as a new cathode material for Ni/MH batteries, because it has good reaction activity, high discharge capacity, good hydrogen storage, low cost, easy activation, and good

chemical stability. It has strong application value, which has aroused widespread attention in related research fields. Chen Yungui's research group [2—4], Liu Yongning's research group [5,6], and Ibrahim AA [7] and Lim's team [8,9] conducted groundbreaking studies on the electrochemical properties of $LaFeO_3$, $LaNiO_3$, and $LaCoO_3$ and their doped systems as electrode materials.

Chen Yungui et al. [4] found that the maximum discharge capacity of the $LaFeO_3$ electrode reaches 625 mAh/g at 80 °C, if the electrode capacity is all contributed by the stored H atoms, and the chemical composition of the oxide is $ABO_3H_5 \sim_6$ according to Faraday's law. However, the hydrogen storage mechanism proposed by Mandal et al. [10] showed that hydrogen can be stored in the O atom of $ABO_3$, when the composition is $ABO_3H_3$. If the hydrogen can also be stored in the O vacancy site, the composition of $ABO_3$ becomes $ABO_{3-\delta}H_{3+\delta}$. However, the results showed that the density of an O vacancy is generally small to a certain extent ($3-\delta \geq 2.6$ [11,12]), and there is a contradiction between the hydrogen storage capacity of $LaFeO_3$ and the maximum discharge capacity (625 mAh/g) in the electrochemical reaction process. Related studies also indicated that the existence of an O vacancy greatly affects the physical and chemical properties of perovskite materials [13—16]. By using the density functional theory (DFT), Zhang et al. [17] found that an O vacancy in $LaAlO_3$ was easily formed on the surface of $AlO_2$. Seo et al. [18] suggested that the $LaAlO_3$ structure was stable in its thermodynamics when the O vacancy existed on the surface of $LaAlO_3(001)$. Zhu et al. [19] found that the presence of O vacancies could lead to an increase in the adsorption energy of H and the charge localization of $LaNiO_3$ to reduce its conductivity. Pavlenko et al. [20] and Lin et al. [21,22] found that an O vacancy has a strong influence on the orbit restructuring of $SrTiO_3$. The O vacancy in the system should be regarded as a magnetic medium, which can affect the magnetic properties of the interface. The progress of the $LaBO_3$ (B= Mn, Fe, Co, Ni) catalytic reduction reaction in solid oxide fuel cells was studied by Lee et al. [23] and Huang et al. [24] by using an ab initio calculation method. They also calculated the formation energies of O vacancies in $LaBO_3$ (B= Mn, Fe, Co, Ni). Rodriguez et al. [25] revealed that the chemical properties of $H_2$ adsorbed on the NiO surface were affected by the O vacancy, and the distribution of O vacancies in the surface and subsurface regions could also be affected by the adsorbate. Sun et al. [26] found that the existence of O vacancy and its occupancy can affect the magnetic exchange between Co ions in Co-doped $TiO_2$. The experiments reported by Wang et al. [27] demonstrated the density of the carriers is enhanced by the O vacancy by one order of magnitude compared with that of the ideal heterojunction $LaGaO_3/SrTiO_3$. Given the results of these investigations, studies on the effects of an O vacancy on hydrogen storage in $LaFeO_3$ are of considerable interest.

To further understand the effects of an O vacancy on the hydrogen storage properties of $LaFeO_3$ surfaces and the hydrogen storage process and adsorption mechanism, this paper, based on the density functional theory (DFT) method, studies the characteristics of the $LaFeO_3$ (010) surface with an O vacancy and the dissociation and adsorption process of $H_2$ molecules at the surface, and it also determines the possible reaction path. It is hoped that this work can provide the

corresponding microscopic mechanism and theoretical data for future experimental studies.

## Computational methods and models

### Calculation parameters

All calculations in this work were performed with the density functional theory using the Cambridge Sequential Total Energy Package (CASTEP) [28] module in Materials Studio (MS) 7.1. By using periodic boundary conditions, the crystal wave function was expanded by the base plane [29]. The exchange-correlation interaction was described by GGA-PBE, which combines the generalized gradient approximation (GGA) and Perdew—Burke—Ernzerhof functional (PBE) [30]. In addition, the ultra-soft pseudopotential (USPP) [31] was used to describe the interaction between electrons and ions.

The $LaFeO_3$ crystal is an orthorhombic perovskite structure with a space group of *Pnma*. In the previous study, we calculated the surface energy of the different surfaces of the $LaFeO_3$ system. According to the surface energy calculation results, the $LaFeO_3$ (010) surface was identified as the most stable adsorption surface [32]. The $LaFeO_3$ (010) surface has two models for the termination of $FeO_2$ and LaO surfaces; however, from the energy point of view, LaO termination surface is difficult to form [33]. In our previous study, it was found that the adsorption and dissociation properties of $H_2$ molecules on the LaO termination surface were poor [33]; therefore, the discussion in this paper was based on the termination of $FeO_2$. To ensure a balanced consideration of the computer calculation ability and calculation reliability, we used a (2 × 2) supercell of 79 atoms to mimic the $LaFeO_3$ (010) surface with an O vacancy. In all cases, the plane-wave expansion was limited to a cutoff energy of 410 eV, the Brillouin zone was sampled with 4 × 4 × 1 k-point grids, the self-consistent field converged to $2.0 \times 10^{-5}$ eV with geometry optimization calculations, and the vacuum thickness was about 20 Å. The structure of the free $H_2$ molecule and $LaFeO_3$ crystal was calculated using the above parameters: the H—H bond length was 0.754 Å, which is in accordance with the experimental value of 0.741 Å [34] and others' calculated value of 0.750 Å [35]. The optimized result showed that the lattice parameters of the $LaFeO_3$ were a = 5.49295 Å, b = 7.75582 Å, and c = 5.5111 Å. They were close to the experimental values of a = 5.55950 Å, b = 7.84980 Å, and c = 5.55090 Å [36]. The results showed that the model was reliable and the selected parameters met the accuracy requirements.

The transition state of the process was also investigated, i.e., the dissociation and adsorption of an $H_2$ molecule on the surface of $LaFeO_3$ (010) with an O vacancy by using the Linear Synergism Transformation (LST) and Quadratic Synergism Transformation (QST) methods [37]. The optimum reaction path and activation energy barrier were simultaneously calculated.

### Location of the O vacancy

The formation of surface energy with an O vacancy can provide a basis for the possibility of vacancy formation in a crystal

structure, and it is an important physical parameter for the study of the structure of materials. The formulas are as follows [38].

$$E_{vf} = E_{vac} - E_0 + \frac{1}{2}\left(E_{O_2} + \Delta h^0_{O_2}\right) \tag{1}$$

where $E_{vac}$ and $E_0$ are the energies of the LaFeO₃ (010) system with O vacancy defects, and the total energy of the complete lattice system, respectively. $E_{O_2}$ is the O₂ molecular energy, and $\Delta h^0_{O_2}$ is an energy correction value for the O₂ molecule, $\Delta h^0_{O_2} = 1.36$ eV/O₂ [39].

Fig. 1(a) indicates the location of the O vacancy in different atomic layers. To be clear and intuitive, only the atoms in the part of the region near the adsorption site are shown, and the other atoms are hidden for the structural diagram of this paper. From Fig. 1(b), the formation energy for the O vacancy in different atomic layers in the LaFeO₃ crystal (the broken line graph), and the O vacancy formation energy in the different atomic layers in the surface structure of LaFeO₃ (the columnar graph) can be seen. The greater the value of vacancy formation energy, the more difficult it is to form an O vacancy [40]. As shown in the diagram, the surface formation energy of the system is lower than that in the cell system, and the formation of an O vacancy on the surface can be smaller than that in the inner layer. Therefore, the surface of the LaFeO₃ (010) system is most likely to form an O vacancy. The O vacancy on the surface of the LaFeO₃ (010) surface system was chosen for the study calculations. The difference in the vacancy formation energy of the crystal and the surface is calculated to be 1.862–2.300 eV, which is consistent with the results of the studies [18] and [38].

## Results and discussion

### Adsorption conditions

First, we calculated the adsorption energy [41] to obtain the stable adsorption site for the H₂ molecule on the LaFeO₃ (010) surface with an O vacancy, which is defined as:

$$E_{ads} = E_{slab/H_2} - \left(E_{clean} + E_{H_2}\right) \tag{2}$$

where $E_{clean}$ is the total surface energy before adsorption and $E_{H2}$ is the total energy of the H₂ molecule. In addition,

$E_{slab/H_2}$ is the total surface energy after adsorption. In this sign convention, negative adsorption energies correspond to the exothermic reaction and the stable configurations. Furthermore, the smaller the adsorption energy, the more stable is the adsorption system.

There are eight possible high-symmetry adsorption sites for the LaFeO₃ (010) surface with an O vacancy: O vacancies sites (V), O—O long bridge sites (B₁), Fe—Fe bridge sites (B₂), Fe—O bridge sites (B₃), O—O short bridge sites (B₄), La top sites (T₁), and Fe—O bridge. Because H₂ molecules are placed in the Fe—O bridge position, the problem of H₂ molecular bond orientation occurs; hence, two cases can be considered: H₂ molecules parallel to the Fe—O bond placed at the O top sites(T₂), and H₂ molecules perpendicular to the Fe—O bond placed at the O top sites (T₃). The results of the calculations, shown in Table 1, represent the adsorption energies and the minimum distance between the H atom and the surface atom after adsorption ($r_{H-H}$, $r_{H-O}$, $r_{H-Fe}$, $r_{H-La}$). The results show that H₂ molecules have four kinds of adsorption modes on a LaFeO₃ (010) surface with an O vacancy. In the first mode, when the H₂ molecule is adsorbed on B4, the H—H bond length increases from 0.754 Å to 3.131 Å and the H₂ molecules are dissociated completely. The dissociative H atoms are adsorbed on the surface of the two O atoms, forming two —OH groups. The - 1.396 eV adsorption energy is less than - 0.415 eV [42], which can be characterized as chemical adsorption. In the second mode, two H atoms are adsorbed on the same O atom to form H₂O when the H₂ molecule is adsorbed on T3; the H—H bond length is 1.640 Å, and the H—O bond length is 0.981 Å. This mechanism is similar to the H₂O molecules' geometric parameters of 1.545 Å and 0.978 Å [43]. The adsorption energy of the H₂ molecule in this position is −0.671 eV, which is a stable chemical adsorption. The results indicate that the adsorption energy of the H₂O molecule on the surface is only −0.250 eV, which can be characterized as physical adsorption. The H₂O molecule is easier to separate from the surface, facilitating the formation of O vacancy defects and resulting in the defect in the crystal surface. In the third mode, H₂ molecules are dissociated and the H—H bond length changes to 2.398 Å and 2.483 Å when the H₂ molecule is adsorbed on the B3 site and T2 site, respectively. The two H atoms are adsorbed on the top of the O and Fe atoms, respectively, forming an —OH group and a Fe—H bond. In addition, the adsorption of the two initial
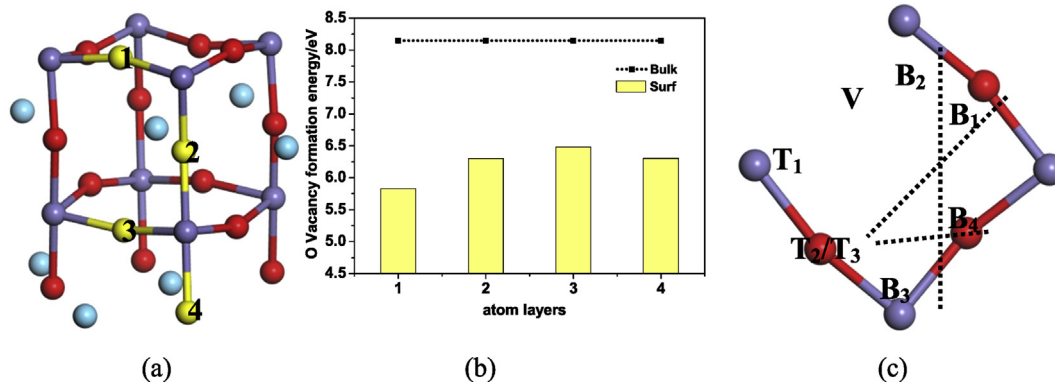


Fig. 1 – LaFeO₃ (010) surface with an O vacancy: (a) the vacancy may be at these locations; (b) O vacancy formation energy relationship; (c) initial adsorption site.

**Table 1 — Energy and geometrical parameters after optimization of LaFeO$_3$ (010)/H$_2$ with an O vacancy and LaFeO$_3$(010)/H$_2$ system.**

| | Initial position | | $r_{H-H}$/Å | $r_{H-O}$/Å | $r_{H-Fe}$/Å | $r_{H-La}$/Å | $E_{ads}$ |
|---|---|---|---|---|---|---|---|
| | V | O vacancy | 0.816 | 2.405 | 1.921 | 2.850 | −0.108 |
| | B$_1$ | O vacancy | 0.757 | 2.345 | 2.683 | 3.400 | −0.134 |
| | B$_2$ | O vacancy | 0.758 | 2.334 | 2.664 | 3.566 | −0.175 |
| Fe−H,−OH | B$_3$ | O vacancy | 2.398 | 0.982 | 1.487 | 3.503 | −0.796 |
| | T$_2$ | O vacancy | 2.483 | 0.981 | 1.476 | 3.446 | −1.095 |
| | | LaFeO$_3$ [32] | 2.305 | 0.978 | 1.482 | 3.159 | −0.826 |
| Fe−H$_2$ | T$_1$ | O vacancy | 0.808 | 2.227 | 1.692 | 4.393 | −0.545 |
| −OH(two) | B$_4$ | O vacancy | 3.131 | 0.978 | 2.476 | 3.089 | −1.396 |
| | | LaFeO$_3$ [32] | 3.294 | 0.978 | 2.542 | 3.131 | −1.866 |
| H$_2$O | T$_3$ | O vacancy | 1.640 | 0.981 | 2.326 | 3.180 | −0.671 |
| | | LaFeO$_3$ [32] | 1.626 | 0.986 | 2.585 | 3.070 | −1.056 |
| | Free H$_2$ | | 0.754 | | | | |
| | H$_2$ [35] | | 0.750 | | | | |
| | H$_2$O [43] | | 1.545 | 0.978 | | | |

positions is considered to be the same adsorption method. The adsorption energy is less than - 0.415 eV, which can be characterized as chemical adsorption. In the last mode, the H−H bond length is elongated slightly but not broken, and the two H atoms are adsorbed on the Fe atom when the H$_2$ molecule is adsorbed on the T1 site. The adsorption energy is - 0.545 eV, which is between physical adsorption and chemical adsorption. In Fig. 2, the schematic diagram for each of the four main adsorption types after geometry optimization calculations is shown. When the H$_2$ molecule is adsorbed on the vacancy and the hollow points (B1, B2, and V), clearly, the state and bond length of H$_2$ do not change after structural optimization, and the adsorption energy is lower than 0 and higher than - 0.415 eV, which is physical adsorption.

In conclusion, there are four kinds of adsorption sites on the LaFeO$_3$ (010) surface with an O vacancy for the adsorption of H atoms after the H$_2$ dissociation. First, H atoms are adsorbed on O atoms to form an −OH group. Second, H atoms are adsorbed on Fe atoms to form Fe−H bonds. Third, two H atoms are adsorbed on the same O atom to form H$_2$O. Fourth, two H atoms are adsorbed on the same Fe atom and it is a new type of adsorption, which does not exist in the ideal surface.

Comparing the adsorption energy and $r_{H-H}$ of the four main adsorption conditions with the defects and the ideal LaFeO$_3$(010)/H$_2$ system, the adsorption energy of the LaFeO$_3$ (010) surface with an O vacancy is obviously larger than the ideal surface when the −OH and Fe−H bonds are formed. In addition, H$_2$ molecules are adsorbed on the Fe top sites, which can form aFe-H$_2$ structure on the LaFeO$_3$ (010) surface with an O vacancy. Therefore, the presence of an O vacancy enhances the adsorption ability of the Fe atom to H, and a surface containing O vacancy defects promotes this adsorption. This conclusion is consistent with the results of Zhu et al., whereby "the presence of an O vacancy leads to an increase in the adsorption energy of H" [19]. In the formation of two-OH structure, the adsorption energy is less than −0.415 eV that is a stable chemical adsorption, indicating that H$_2$ molecules can be a stable adsorption in the B4 position, H atoms and the surface of the O atoms to form covalent bonds. In the ideal surface, the adsorption energy at this position is −1.866 eV [32], which are stronger than that on the defect surface. It can be seen that strong covalent bond is formed between H and O atoms. On the contrary, it is difficult to separate the H atoms from the adsorbed surface, that is, it is not easy to release



-OH(two)          H$_2$O          Fe-H，-OH          -H$_2$
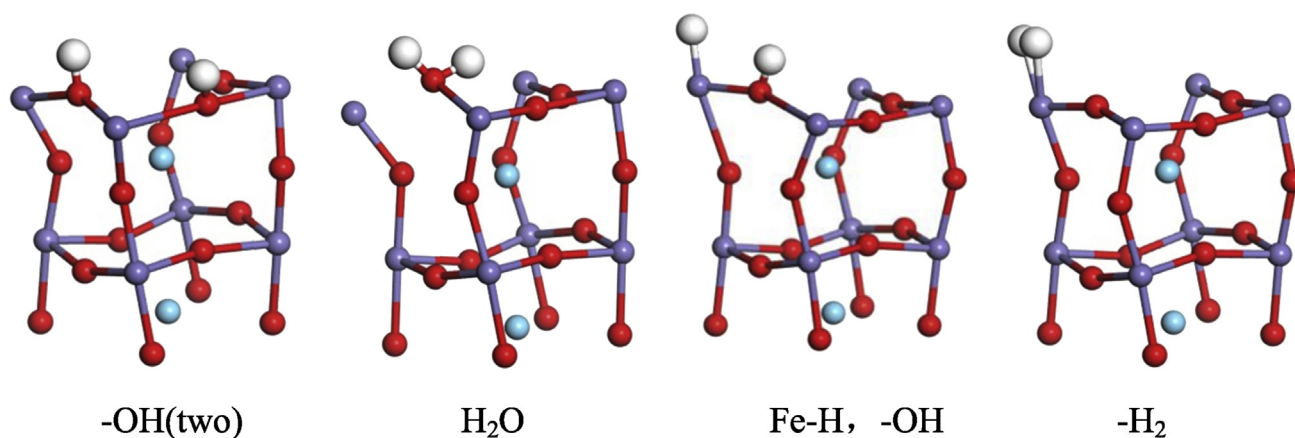
**Fig. 2 — Four main adsorption positions shown in structural schematics after geometry optimization calculations.**

hydrogen. In this paper, the adsorption properties of $H_2$ molecules on the surface of defect $LaFeO_3$ (010) are studied, but the rationality of hydrogen release in later studies is also taken into account. Therefore, the $LaFeO_3$ (010) surface system with O vacancy is more suitable as a hydrogen storage material than the ideal surface. If the O atom and Fe atom could store hydrogen in the defect surface system, the relationship between the hydrogen storage capacity and discharge capacity of the $LaFeO_3$ system could be explained [4].

### Chemical processes of dissociation and adsorption of $H_2$

To study the dissociation and adsorption process of $H_2$ on the $LaFeO_3$ (010) surface with an O vacancy, the structure of the $H_2$ molecule is placed on the surface of B4, T3, and T2 in the initial state, and the optimized version is the final state. As shown in Table 2, the transition state, activation energy barrier, and reaction energy of the three chemical adsorption processes can be calculated. It can be seen that the activation energy barrier exists in the three kinds of adsorption and dissociation processes, which means that the reaction experiences some difficulty in spontaneous occurrence, and external conditions are needed to stimulate these reactions. The activation energy barrier of −OH and Fe−H is the lowest, which indicates that the reaction can easily occur. To simulate adsorption of the H atoms on the surface, the most stable adsorption sites on the surface of the H atoms were found to be the O top sites, and the adsorption of the H atom at the top of the Fe to the O top must overcome the energy barrier of 0.794 eV. Compared with the diffusion energy barrier of H atoms diffused from Fe to O atoms in the ideal surface (0.968 eV) [32], the defect surface is more likely to diffuse the H atoms to the most stable adsorption sites, and also make the material easier to hydrogen. It is concluded that there are two paths for $H_2$ molecules to dissociate and adsorb and diffuse to the most stable adsorption sites (O-top). The stepwise pathways are $H_2$ molecules to dissociate to form −OH and Fe−H structures, and then the H atoms adsorbed on Fe diffuse to the most stable adsorption sites O, the total energy required for both processes is 1.377 eV; The direct path is that $H_2$ molecules directly dissociate and adsorb to form two-OH groups with a barrier of 4.591 eV. It can be seen that the energy barrier of the step path is significantly smaller than the energy barrier of the direct path. Therefore, the formation of the −OH and Fe−H structures is considered to be the main adsorption mode for the $H_2$ molecule, and there is no competition between the three adsorption methods. To understand the adsorption mechanism, the characteristics of charge transfer and bonding in the

main adsorption methods are further calculated and analyzed.

### Adsorption mechanism of $H_2$

#### Charge population

The charge population can be used to quantitatively analyze the bond strength between the atoms. The interaction between the H atoms and the surface atoms can be obtained according to the charge distribution before and after adsorption. Table 3 lists the Mulliken charge population before and after adsorption. It can be seen that the s and p orbital charge values of the atoms exhibit a larger difference after adsorption; the H atoms connected with the O atoms lose electrons (0.38 e), and the O atoms gain electrons (0.16 e). The H atom connected with the Fe atom has an electron (0.18e) [32], and in the ideal surface model without an O vacancy, the electron number of the H atom connected with Fe is 0.16e, which shows that the presence of an O vacancy enhances the adsorption capacity of the Fe atom to H. Table 4 lists the bond population numbers and bond length of the system before and after adsorption. The bond population numbers between O−La and O−Fe is decreased and the bond length is larger after adsorption, which indicates that the interaction between O−La and O−Fe decreases. In the ideal $LaFeO_3$ surface adsorption model, the number of bonds between H−Fe is 0.58 e [32], and the electron number of H−Fe in the defect model is 0.61 e. This phenomenon also indicates that the adsorption of Fe atoms to H is enhanced by the presence of O vacancies.

#### Electron localization function

The electron localization function (ELF) is a powerful tool to investigate the charge transfer, which reflects the localization of electrons in the crystal structure and the relative chemical bond strength. It is often used to analyze the bonding type between atoms in a system [44]. By observing the function of the electron local value in the gap between the atoms, bond types can be judged qualitatively. According to the definition of ELF, which has a range of 0−1, when $0.75 < ELF \leq 1$, the electrons are highly localized and exhibit strong covalent bonds; moreover, this is realized for a metal bond when $0.5 \leq ELF \leq 0.75$. This area belongs to a weaker electric area, which shows a strong ionic bond when $0 \leq ELF < 0.5$. Fig. 3 shows the distribution of the electron density at the most stable adsorption position after optimization. The region between the H atom and O atom is red, and the ELF value is close to 1, thus proving the typical feature of a covalent bond. In contrast, the orange area shown in Fig. 3 is the area between the H and Fe atoms, and the ELF value is about 0.75, which demonstrates evidence of a metallic bond.

#### Density of states

The density of states (DOS) for the system can show the number of states in the unit energy interval. To study the bonding interaction between the H atoms and the atoms at the surface, we compared their DOS. The DOS of the $H_2$ molecule adsorption on the most stable adsorption site before and after adsorption (the energy zero position as the

| Table 2 − Energy parameters for the three kinds of chemical adsorption. | | | |
|---|---|---|---|
| | Barrier from reactant/eV | Barrier from product/eV | Energy of reaction/eV |
| $H_2O$ | 2.989 | 3.206 | −0.217 |
| Fe−H, −OH | 0.583 | 1.386 | −0.803 |
| −OH | 4.591 | 5.625 | −1.034 |

**Table 3 – Charge distribution variation in the most stable adsorption sites before and after adsorption.**

| | Before adsorption/e | | | | After adsorption/e | | | |
|---|---|---|---|---|---|---|---|---|
| | s | p | d | Charge | s | p | d | Charge |
| $H_1$ | 1.0 | | | | 0.62 | | | 0.38 |
| $H_2$ | 1.0 | | | | 1.18 | | | −0.18 |
| $O_1$ | 1.87 | 4.85 | | −0.72 | 1.87 | 4.84 | | −0.71 |
| $O_2$ | 1.88 | 4.76 | | −0.63 | 1.86 | 4.93 | | −0.79 |
| $Fe_3$ | 0.35 | 0.50 | 6.49 | 0.66 | 0.36 | 0.49 | 6.52 | 0.63 |
| $Fe_{12}$ | 0.36 | 0.52 | 6.51 | 0.61 | 0.39 | 0.42 | 6.58 | 0.62 |
| $La_{12}$ | 2.17 | 5.99 | 1.28 | 1.56 | 2.17 | 5.99 | 1.29 | 1.54 |

**Table 4 – Bond population and bond length variation in the most stable adsorption sites before and after adsorption.**

| Bond | Population/e | | Length/Å | |
|---|---|---|---|---|
| | Before ads. | After ads. | Before ads. | After ads. |
| $H_1–O_2$ | | 0.64 | | 0.981 |
| $H_2–Fe_{12}$ | | 0.61 | | 1.476 |
| $O_1–La_{12}$ | 0.15 | 0.13 | 2.369 | 2.441 |
| $O_2–Fe_3$ | 0.45 | −0.01 | 1.881 | 2.807 |
| $O_2–Fe_{12}$ | 0.60 | 0.34 | 1.806 | 1.882 |

Fermi level) is shown in Fig. 4. The figure shows that the highest occupied state of the crystal is in the energy range of −7.4–3.7 eV, which shows contributions from the O 2p orbital and Fe 3d orbital hybridization. In addition, the highest occupied state moves to the deep level after adsorption. Thus, the H atoms and the surface interactions are very strong. The DOS of H splits after adsorption, which indicates that the $H_2$ molecules have been dissociated. In addition, the interaction mainly occurs between the O atoms and Fe atoms at the surface and the H atoms. The H 1s orbital and the O 2p orbital are obviously split and broadened. There are some obvious overlaps and resonance, which indicates that the covalent bond between H and O is formed. After the adsorption of H, the DOS of the Fe atom is changed, and the main change occurs in the Fe 3d orbit. The highest occupied state of the Fe 3d orbit is in the −8.0–3.2 eV energy region after adsorption, which is higher than the −7.2–3.0 eV energy region before adsorption. At the same time, the peak value increases obviously, which indicates the reaction between the H atom and the Fe atom. After the
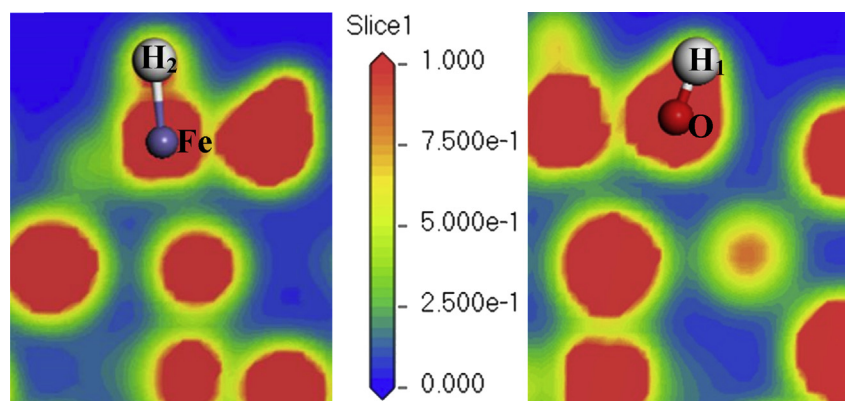


Fig. 3 – Electron localization function graph of the most stable adsorption sites after adsorption.
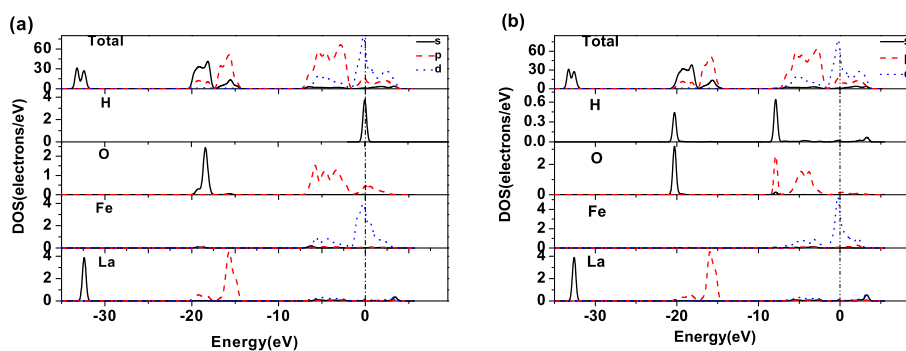


Fig. 4 – Density of states of the most stable adsorption site before and after adsorption: (a) before adsorption;(b) after adsorption.

adsorption of H atoms, the DOS of the La atoms exhibit no significant changes.

## Conclusion

1) In calculating the vacancy formation energy at the $LaFeO_3$ (010) surface and cell, it was found that an O vacancy is more easily formed on the surface.

2) It was confirmed that $H_2$ molecules have four kinds of adsorption modes on the $LaFeO_3$ (010) surface with an O vacancy. The first adsorption mode is that the $H_2$ molecules are completely dissociated and adsorbed onto two different O atoms to form the two −OH groups. Second, the two H atoms are adsorbed onto an O atom, forming $H_2O$. Third, the $H_2$ molecule is dissociated and an H atom is adsorbed onto an O atom to form −OH, where H−O is a covalent bond; another H atom is adsorbed onto a Fe atom to form an Fe−H metal bond, which is the main channel of dissociation and adsorption. The fourth adsorption mode is a mechanism between physical adsorption and chemical adsorption, and finally forms an $FeH_2$ structure. A physical adsorption reaction may also simultaneously occur.

3) With the presence of O vacancies, the hydrogen absorption capacity of Fe atoms in $LaFeO_3$ is improved, and the interaction between Fe−H is enhanced. In the system containing O vacancies, adsorbed H atoms in the top of Fe to diffuse to the top of O need to overcome the energy barrier decreased from 0.968eV to 0.794eV, which also leads to an improvement in the absorption performance of H.

4) When the $H_2$ molecule is adsorbed to form $H_2O$, the $H_2O$ molecule can more easily break away from the defect surface containing an O vacancy, thus forming an O vacancy again, which leads to the defect on the crystal surface.

REFERENCES

[1] Bäuerlein P, Antonius C, Löffler J, Kümpers J. Progress in high-power nickel–metal hydride batteries. J Power Sources 2008;176(2):547–54.

[2] Wang Q, Deng G, Chen Z, Chen Y, Cheng N. Electrochemical hydrogen property improved in nano-structured perovskite oxide $LaFeO_3$ for Ni/MH battery. J Appl Phys 2013;113(5). 053305-5.

[3] Deng G, Chen Y, Tao M, Wu C, Shen X, Yang H, et al. Electrochemical properties and hydrogen storage mechanism of perovskite-type oxide $LaFeO_3$ as a negative electrode for Ni/MH batteries. Electrochim Acta 2010;55(3):1120–4.

[4] Deng G, Chen Y, Tao M, Wu C, Shen X, Yang H, et al. Preparation and electrochemical property of $LaFeO_3$ electrode material (in Chinese). Hua Hsueh Hsueh Pao 2009;67(17):2001–4.

[5] Liu Y, Liu Y, Ma J, Lai J. $La_{1-x}Sr_xCoO_3$ (x = 0.1-0.5) as the cathode catalyst for a direct borohydride fuel cell. J Power Sources 2010;195(7):1854–8.

[6] Ma J, Liu Y, Liu Y, Yan Y, Zhang P. A membraneless direct borohydride fuel cell using $LaNiO_3$-catalysed cathode. Fuel Cell 2008;8(6):394–8.

[7] Ibrahim AA. Hydrogen storage in proton-conductive perovskite-type oxides and their application. Kor J Chem Eng 2014;31(10):1792–7.

[8] Lim DK, Im HN, Singh B, Park CJ, Song SJ. Electrochemical hydrogen charge and discharge properties of $La_{0.1}Sr_{0.9}Co_{1-y}Fe_yO_{3-\delta}$(y=0, 0.2, 1) electrodes in alkaline electrolyte solution. Electrochim Acta 2013;102:393–9.

[9] Lim DK, Im HN, Kim J, Song SJ. Electrochemical properties of $LaMO_3$ (M=Co or Fe) as the negative electrode in a hydrogen battery. J Phys Chem Solid 2013;41(1):115–20.

[10] Mandal TK, Sebastian L, Gopalakrishnan J, Abrams L, Goodenough JB. Hydrogen uptake by barium manganite at atmospheric pressure. Mater Res Bull 2004;39(14):2257–64.

[11] Wang ZL, Kang ZC, Uchino K. Functional and smart materials: structural evolution and structural analysis. Phys Today 1998;51(11):70–1.

[12] Patrakeev MV, Bahteeva JA, Mitberg EB, Leonidov A, Kozhevnikov VL, Poeppelmeier KR. Electron/hole and ion transport in $La_{1-x}Sr_xFeO_{3-\delta}$. J Solid State Chem 2003;172(1):219–31.

[13] Peña MA, Fierro JL. Chemical structures and performance of perovskite oxides. Chem Rev 2001;101(7):1981–2017.

[14] Frantzeskakis E, Avila J, Asensio MC. A chemical imaging and Nano-ARPES study of well-ordered thermally reduced $SrTiO_3$(100). Phys Rev B 2012;85:125115–6.

[15] Adachi G, Imanaka N, Tamura S. Ionic conducting lanthanide oxides. Chem Rev 2002;102(6):2405–30.

[16] Astala R, Bristowe PD. Ab initio and classical simulations of defects in $SrTiO_3$. Comput Mater Sci 2001;22(1–2):81–6.

[17] Zhang L, Zhou XF, Wang HT, Xu JJ, Li J, Wang EG, et al. Origin of insulating behavior of the p-type $LaAlO_3$/$SrTiO_3$ interface: polarization-induced asymmetric distribution of oxygen vacancies. Phys Rev B 2010;82(12):2951–7.

[18] Seo H, Demkov AA. First-principles study of polar $LaAlO_3$ (001) surface stabilization by point defects. Phys Rev B 2011;84(4), 045440.

[19] Zhu MW, Wang HL, Han HJ, Wang ZJ, Zhang ZD. Effect of interface structure on the chemical composition and electrical properties of sol−gel-derived $LaNiO_3$ films. Appl Phys A 2015;119(3):949–55.

[20] Pavlenko N, Kopp T, Tsymbal EY, Sawatzky GA, Mannhart J. Magnetic and superconducting phases at the $LaAlO_3$/$SrTiO_3$ interface: the role of interfacial Ti 3d electrons. Phys Rev B 2012;85(2):235–40.

[21] Lin C, Mitra C, Demkov AA. Orbital ordering under reduced symmetry in transition metal perovskites: oxygen vacancy in $SrTiO_3$. Phys Rev B 2012;86(16):755–9.

[22] Lin CW, Demkov AA. Electron correlation in oxygen vacancy in $SrTiO_3$. Phys Rev Lett 2013;111(21):217601–5.

[23] Lee YL, Morgan D, Kleis J, Rossmeisl J. Ab initio defect energetics in $LaBO_3$ perovskite solid oxide fuel cell materials. ECS Trans 2009;25(2):2761–7.

[24] Huang WL, Zhu Q, Ge W, Li H. Oxygen-vacancy formation in $LaMO_3$ (M = Ti, V, Cr, Mn, Fe, Co, Ni) calculated at both GGA and GGA plus U levels. Comput Materialsence 2011;50(5):1800–5.

[25] Rodriguez JA, Hanson JC, Frenkel AI, Kim JY, Pérez M. Experimental and theoretical studies on the reaction of $H_2$ with NiO: role of O vacancies and mechanism for oxide reduction. J Am Chem Soc 2002;124(2):346–54.

[26] Sun YB, Zhang XQ, Li GK, Yang HT, Cheng ZH. Effects of oxygen vacancy on impurity distribution and exchange interaction in Co-doped $TiO_2$. Acta Phys Sin 2012;61(2). 027503-027503.

[27] Wang FN, Li JC, Zhang XM, Liu HZ, Liu J, Wang CL, et al. Electrical property effect of oxygen vacancies in the heterojunction of $LaGaO_3$/$SrTiO_3$. Chin Phys B 2017;26(3):436–40.

[28] Segall MD, Lindan PJD, Probert MJ, Pickard CJ, Hasnip PJ, Clark SJ, et al. First-principles simulation: ideas, illustrations and the CASTEP code. J Phys Condens Matter 2002;14:2717–44.

[29] Pan CC, Chen YH, Wu N, Zhang ML, Yuan LH, Zhang CR. A first principles study of $H_2$ adsorption on $LaNiO_3$ (001) surfaces. Materials 2017;10(1):1–13.

[30] Perdew JP, Burke K, Ernzerhof M. Generalized gradient approximation made simple. Phys Rev Lett 1996;77(18):3865–8.

[31] Vanderbilt D. Soft self-consistent pseudopotentials in a generalized eigenvalue formalism. Phys Rev B 1990;41(11):7892–5.

[32] Chen YH, Pan CC, Zhang ML, Yuan LH, Zhang CR, Kang L, et al. First principles study on the adsorption of $H_2$ molecules on $LaFeO_3$ surface. Chin J Inorg Chem 2016;32(6):945–53.

[33] Sun LH, Hu JF, Gao F, Zhang YJ, Qin HW. First-principle study of NO adsorption on the $LaFeO_3$ (010) surface. Phys B Phys Condens Matter 2011;406(21):4105–8.

[34] Íñiguez J, Yildirim T, Udovic TJ, Sulic M, Jensen CM. Structure and hydrogen dynamics of pure and Ti-doped sodium alanate. Phys Rev B 2004;70(6):060101–4.

[35] Kresse G, Hafner J. First-principles study of the adsorption of atomic H on Ni (111), (100) and (110). Surf Sci 2000;459(3):287–302.

[36] Taguchi H, Masunaga Y, Hirota K, Yamaguchi O. Synthesis of perovskite-type $(La_{1-x}Ca_x)$ $FeO_3$ ($0 \leq x \leq 0.2$) at low temperature. Mater Res Bull 2005;40(5):773–80.

[37] Bell S, Crighton JS. Locating transition states. J Chem Phys 1984;80(6):2464–75.

[38] Lee YL, Kleis J, Rossmeisl J, Morgan D. Ab initio energetics of $LaBO_3$ (001) (B=Mn, Fe, Co, and Ni) for solid oxide fuel cell cathodes. Phys Rev B 2009;80(22):308–10.

[39] Wang L, Maxisch T, Ceder G. Oxidation energies of transition metal oxides within the GGA+U framework. Phys Rev B 2006;73(19). 195107-5.

[40] Pan CC, Chen YH, Wu N, Zhang ML, Yuan LH, Zhang CR. First-principle study of O vacancy on $LaNiO_3$ (001) surface. Int J Hydrogen Energy 2016;41(35):15756–63.

[41] Alfonso DR. First-principles studies of $H_2S$ adsorption and dissociation on metal surfaces. Surf Sci 2008;602(16):2758–68.

[42] Luo WH, Meng DQ, Li G, Chen HC. Density functional study of CO adsorption on Pu (100) surface. Acta Phys Sin 2008;57(1):160–4.

[43] Evans MW, Refson K, Swamy KN, Lie GC, Clementi E. Molecular-dynamics simulation of liquid water with an ab initio flexible water-water interaction potential. II. The effect of internal vibrations on the time correlation functions. Phys Rev 1987;36(8):3935–42.

[44] Wang XY, Chen NK, Wang XP, Zhang B, Chen ZH, Li XB, et al. Bonding nature of the amorphous structure studied by a combination of cutoff and electronic localization function. Acta Phys Sin 2016;65(17):173101–4.